

Tactile Sensing Device Instantaneously Evaluating Friction Coefficients

Katsuhiko Nakamura* and Hiroyuki Shinoda**

*Tokyo University of Agriculture & Technology, 2-24-16 Koganei, Tokyo 184-8588 Japan

**The University of Tokyo, 7-3-1 Hongo, Bunkyo-ku, Tokyo 113-0033 Japan
shino@alab.t.u-tokyo.ac.jp

Abstract

A human can lift up an object with the almost minimum grasping force regardless of the friction coefficient between the fingers and the object, but the sensing mechanism for this remarkable task has not been well explicated yet. Last year we proposed a tactile sensing principle to detect a friction coefficient at the moment of touching. But we had not reached yet to make a real sensor. In this paper we present a structure of the sensor that was created since then and show successful results of the friction coefficient detection.

Keywords: tactile Sensor, haptic interface, friction coefficient, grasping.

INTRODUCTION

It is known that a human can lift up an object with almost minimum grasping force regardless of the friction coefficient between the fingers and the object [1], but the sensing mechanism for this remarkable task has not been well explicated yet. One strategy to mimic this task in robotics is pre-perception of the friction coefficient by rubbing an object with the finger before grasping. Another approach is to detect dynamic signals [2] arising at slip outsets.

Meanwhile we proposed a tactile sensor that detects friction coefficient at the moment of touching [3]. We showed a theory and numerical calculation results suggesting that the friction coefficient between a sensor and an object is detected by sensing vertical and horizontal stress in a sensor skin simultaneously, without any preliminary motions. But we had not confirmed the principle using a real sensor yet. In this paper we propose a sensor structure using ARTC tactile sensing element [4] and show successful results of the friction coefficient detection.

Using this sensor we would be able to realize the “minimum force grasping” simply by gradually increasing both the grip force and lift force according to the sensor signal.

SENSING PRINCIPLE

Suppose a tactile sensor has a sensing element that detects both vertical and horizontal strain. See Fig. 1. When a rigid object is pressed on the sensor as shown in

Fig. 1, the deformation of the sensor under the contact area depends on the friction coefficient.

Case 1: If the friction coefficient is zero, the sensor skin extends horizontally, and small slips arise overall the contact area. See Fig. 1 (b-2).

Case 2: If the friction coefficient is sufficiently large, the skin can not move horizontally, and a shearing stress distribution $T_s(x)$ arises as shown in

Fig. 1 (b-1).

FEM results for finite friction coefficients μ , shows horizontal stress under the surface changes continuously as the μ changes [3] unless μ is much larger than 1. This result tells us if we sense the horizontal stress under a contact area, we can estimate the friction coefficient.

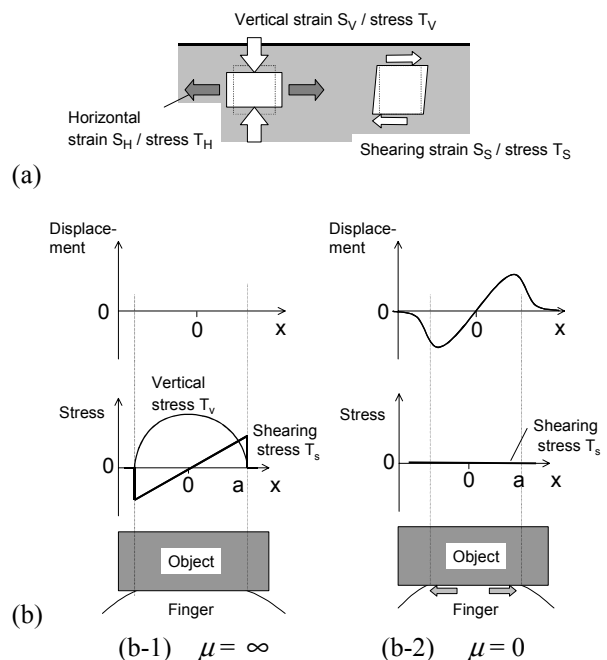


Fig. 1: (a): The terminology of stress/strain component in this paper. (b): Deformation and shearing stress when a finger (tactile sensor) touches an object vertically.

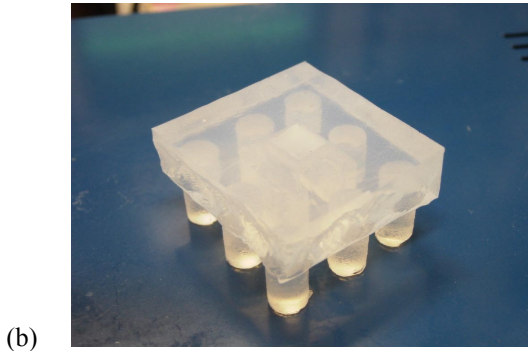
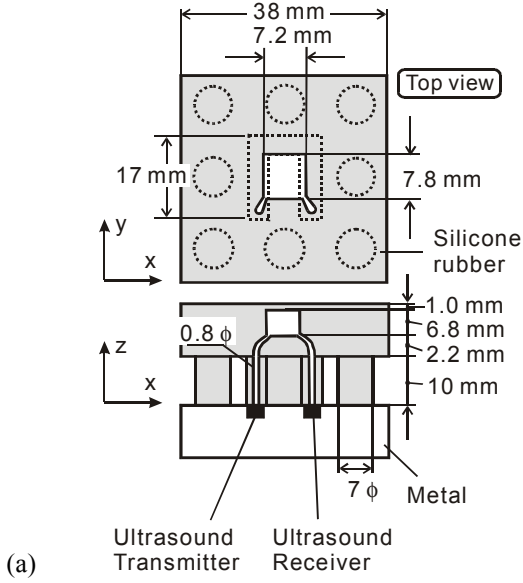


Fig. 2: The sensor structure with an ARTC. The sensor body is made of transparent silicon rubber.

STRUCTURE OF THE SENSOR

Fig. 2 shows the structure of the sensor. An elastic body has a tactile sensing element called “Acoustic Resonant Tensor Cell” (ARTC) [4]. The ARTC is a parallelepiped cavity in the sensor skin connected to an airborne ultrasound transmitter and receiver. From the three primary acoustic resonant frequencies of the cavity air, it detects the extension of the cavity along the edges. The skin is sustained by nine projections as the figure shows in order to make the horizontal constraint to the elastic body under the cavity free.

RESONANT FREQUENCY DETECTION

After stopping the emission from the ultrasound transmitter that excites the cavity air, we observe a relaxation signal as shown in **Fig. 3** by the ultrasound receiver when the excitation frequency is close to the resonant frequencies. The frequency of the relaxation signal is always equal to the resonant frequency of the cavity air regardless of the excitation frequency while the amplitude depends on the excitation frequency.

Fig. 4 shows the amplitude of the relaxation signal versus the excitation frequency. The excitation signals are 2 ms burst with constant amplitude. Three peaks corresponding to the three primary resonant modes are seen. The three frequencies indicate the lengths of the three edges of the parallelepiped cavity. We estimate the vertical cavity extension ratio u_V as

$$u_V = -\frac{\Delta f_3}{f_3} \quad (1)$$

and the horizontal cavity extension ratio along x axis u_H (See **Fig. 2** (a)) as

$$u_H = -\frac{\Delta f_1}{f_1} \quad (2)$$

The sampling of the tactile signal is done as follows. We excite the cavity air at the resonant frequency measured in the previous sampling. A computer calculates the frequency of the relaxation signal after AD converting. This process is done three times sequentially for the three resonant modes. Sampling time (the time to obtain all three frequencies) in the current system is 0.39 sec. Theoretically the minimum sampling time to obtain one resonant frequency is several milliseconds that is the duration of the relaxation signal.

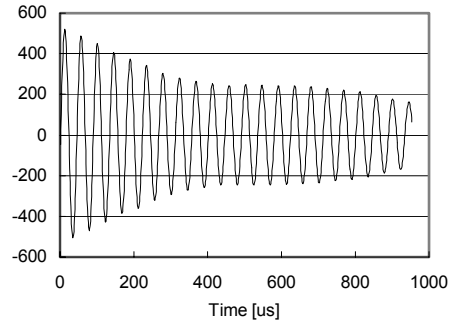


Fig. 3: Relaxation signal of the 22.5 kHz f_1 mode.

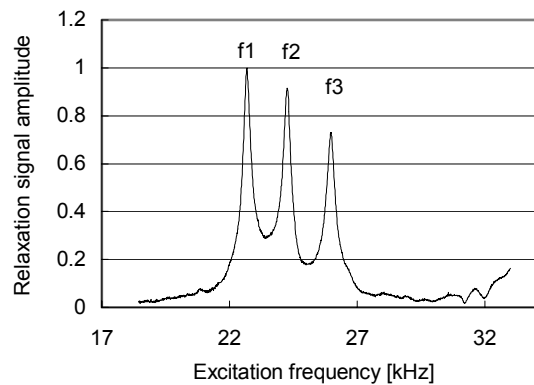


Fig. 4: Three primary resonant frequencies f_1 , f_2 , and f_3 corresponding to the three edges of the parallelepiped. f_1 and f_2 are those of the horizontal modes, and f_3 the vertical mode.

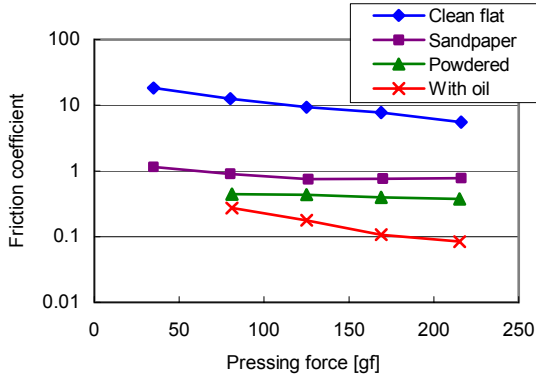


Fig. 5: Friction coefficients versus vertical contact force. The friction coefficients between the sensor and hard flat objects covered with a sandpaper, powder and oil were, respectively, about 0.8, 0.4, and 0.1 when the applied contact force to the sensor was 100 gf ~ 200 gf.

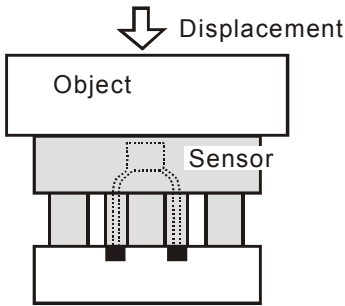


Fig. 6: View of the experiment.

EXPERIMENTAL RESULTS

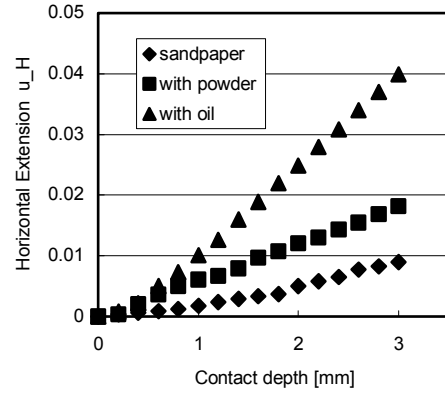
Fig. 7 shows the measured extensions u_H and u_V of the ARTC cavity when three kinds of objects are pressed on the sensor vertically as is shown in **Fig. 6**. All the three objects have flat and rigid surfaces, but they are given different frictional properties by being covered with a sandpaper, powder, and oil, respectively. The characteristics of the friction are shown in **Fig. 5**.

The horizontal extension of the cavity u_H derived from the resonant frequency f_1 , clearly depends on the friction coefficient. Next we evaluate the influences of contact speed, contact angle, and surface curvature on the friction estimation.

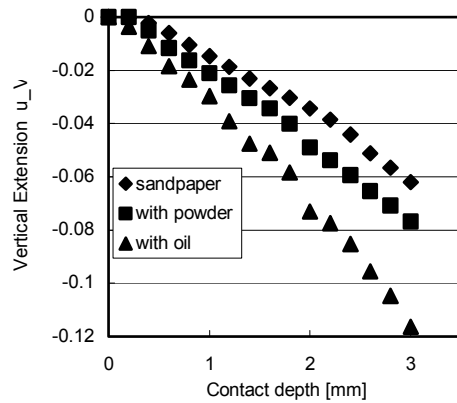
As is seen in **Fig. 7**, the horizontal/vertical cavity extension is proportional to the contact depth. Therefore the ratio

$$R = u_V / u_H \quad (3)$$

is independent of the contact depth. Then we observed the ratio R in various contact motions for the three kinds of objects. **Fig. 9** shows plots of R when we pressed the sensor at three kinds of speed 0.8, 0.38, and 0.18 mm/s, respectively.



(a)



(b)

Fig. 7: Measured extension u_H and u_V of the cavity when we pressed various surfaces on the sensor. (a): horizontal extension ratio u_H calculated by Eq. (2), and (b): vertical extension ratio u_V .

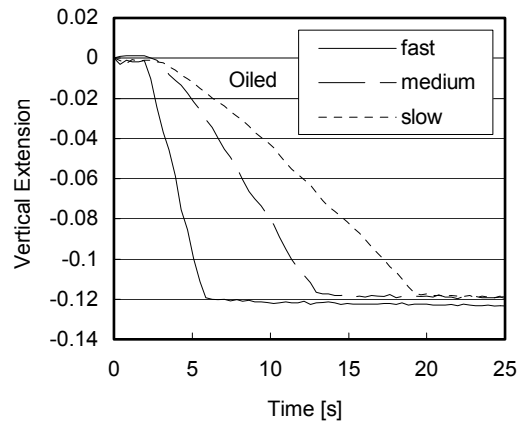


Fig. 8: Vertical extension u_V by three types of (vertical) contact speeds fast (0.8 mm/s), medium (0.38 mm/s) and slow (0.18 mm/s), respectively.

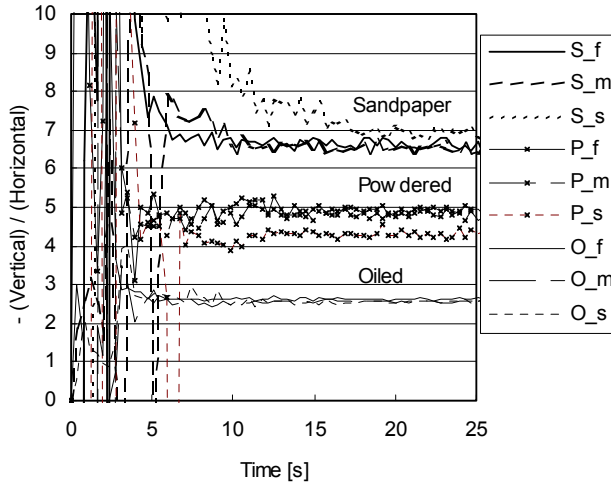


Fig. 9: Plots of R in Eq. (3) by various objects and contact speeds. The capital letters S, P, and O mean the object surfaces covered with a sandpapers, powdered, and oiled, respectively. The small letters f, m, and s mean the contact speeds, fast (0.8 mm/s), medium (0.38 mm/s), and slow (0.18 mm/s), respectively.

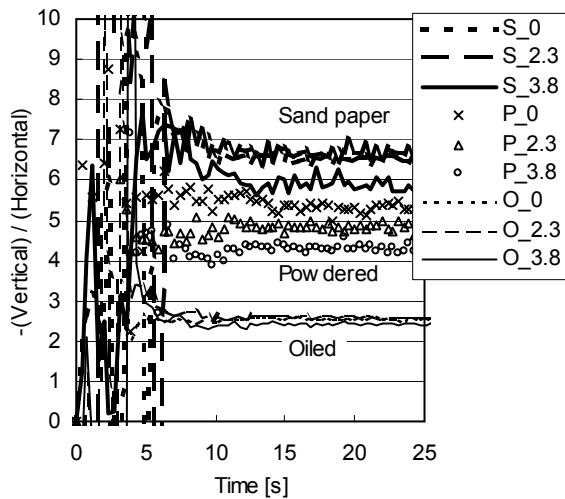


Fig. 10: Plots of R for inclined surfaces. “S_2.3” means the sandpaper surface inclined at 2.3 degree around the x axis.

The three motions are illustrated in **Fig. 8** by u_V measured during the contact motions. The maximum contact depth was 3 mm that corresponded to $u_V = -0.12$. The experimental results in **Fig. 9** showed the three types of frictional properties were distinguishable from R regardless of the pressing speeds.

Fig. 10 shows plots of R for inclined surfaces. This figure shows the sensor output is not very sensitive to the inclination of the object surface. **Fig. 11** shows R s for a curved surface with a curvature radius 10 cm. For

a curved surface, the ability of the friction sensing is largely lost. In order to obtain stable sensation, a sensor is required to have a structure like a human finger that allows to create uniform contact pressure distribution, even to a curved surface of an object. But for flat surfaces, these results show it is possible to estimate the friction coefficient μ from the horizontal and vertical extension of the ARTC cavity when μ is smaller than 1.

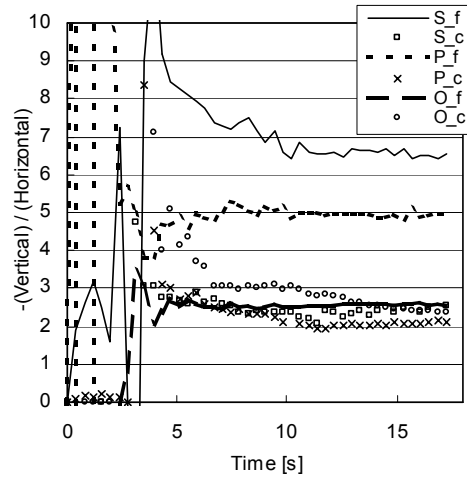


Fig. 11: Comparison between R s for flat surfaces and those for curved surfaces with a curvature radius 10 cm. The small capitals f and c mean flat and curved, respectively. The capital letters S, P, and O mean the object surfaces covered with a sandpapers, powdered, and oiled, respectively.

References

- [1] R.S. Johansson and G. Westling, “Roles of Glabrous Skin Receptors and Sensorimotor Memory in Automatic Control of Precision Grip when Lifting Rougher or More Slippery Objects,” *Exp. Brain Res.*, 56, pp.550-564, 1984.
- [2] M. R. Tremblay and M. R. Cutkosky, “Estimating Friction Using Incipient Slip Sensing During a Manipulation Task,” *Proc. 1993 IEEE Int. Conf. on Robotics & Automation*, pp. 429-434, 1993.
- [3] H. Shinoda, S. Sasaki, and K. Nakamura, “Instantaneous Evaluation of Friction Based on ARTC Tactile Sensor,” *Proc. 2000 IEEE Int. Conf. on Robotics and Automation*, pp.2173-2178, 2000.
- [4] H. Shinoda, K. Matsumoto and S. Ando, “Tactile Sensing Based on Acoustic Resonance Tensor Cell,” *Proc. TRANSDUCERS '97*, Vol. 1, pp. 129-132, 1997.